IOP PUBLISHING JOURNAL OF PHYSICS: CONDENSED MATTER

J. Phys.: Condens. Matter **19** (2007) 406223 (9pp) doi:10.1088/0953-8984/19/40/406223

Crystal structure and the Mott–Hubbard gap in $YTiO_3$ at high pressure

I Loa[1,5], X Wang[1], K Syassen[1], H Roth[2], T Lorenz[2], M Hanfland[3] and Y-L Mathis[4]

[1] Max-Planck-Institut für Festkörperforschung, Heisenbergstrasse 1, D-70569 Stuttgart, Germany
[2] Universität zu Köln, II. Physikalisches Institut, Zülpicher Strasse 77, D-50937 Köln, Germany
[3] European Synchrotron Radiation Facility, BP 220, F-38043 Grenoble, France
[4] ANKA/ISS, Forschungszentrum Karlsruhe, PF 3640, D-76021 Karlsruhe, Germany

E-mail: I.Loa@ed.ac.uk

Received 28 May 2007, in final form 6 August 2007
Published 21 September 2007
Online at stacks.iop.org/JPhysCM/19/406223

Abstract

The crystal structure of $YTiO_3$ at high pressures up to 30 GPa has been investigated by means of synchrotron x-ray powder diffraction ($T = 295$ K). The variation of the Ti–O bond lengths with pressure evidences a distinct change in the distortion of the TiO_6 octahedra at around 10 GPa, which is discussed in terms of a pressure-driven spatial reorientation of the occupied Ti $3d(t_{2g})$ orbitals. Mid-infrared synchrotron microspectroscopy has been used to determine quantitatively the pressure-induced reduction of the optical bandgap of $YTiO_3$, and the results are interpreted on the basis of the structural and possible orbital orientation changes.

1. Introduction

Orbital ordering, fluctuation and excitation phenomena of 3d electrons in transition metal perovskites have attracted much interest. For e_g electron systems like $LaMnO_3$ (electron configuration $3d^4(t_{2g}^3e_g^1)$), the lifting of energetic degeneracies due to lattice distortions (Jahn–Teller effect) and concomitant spatial ordering of the occupied e_g orbitals are well known. In contrast, the t_{2g} states in systems like rare-earth titanates (configuration $3d^1(t_{2g}^1)$) have often been assumed to be degenerate and thus to disfavor orbital ordering. $YTiO_3$ (figure 1(a)) is a prototypical Mott–Hubbard insulator with ferromagnetic ground state, where the question of t_{2g} orbital ordering has been studied in some detail. Static ordering was predicted theoretically [1, 2] and confirmed in nuclear magnetic resonance [3] and several other experiments [4–8]. The mechanism and energetics of the ordering were investigated in theoretical studies [9–13]. In contrast to these experimental and theoretical findings, the

[5] Author to whom any correspondence should be addressed. Present address: The University of Edinburgh, School of Physics and CSEC, Edinburgh, UK.

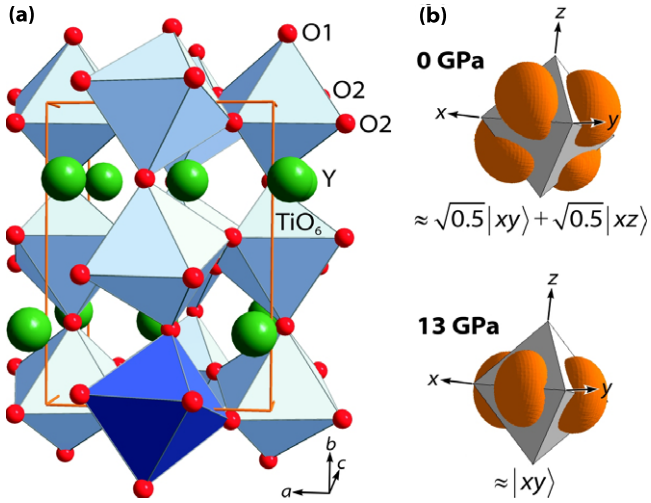

Figure 1. (a) Perovskite-type ($GdFeO_3$) crystal structure of $YTiO_3$ (space group *Pnma*) [31]. (b) Orientation of the titanium $3d^1(t_{2g})$ wavefunction at 0 and 13 GPa as derived in this work from the TiO_6 octahedral distortion. The orbitals shown refer to the Ti site highlighted in (a). The octahedra in (b) illustrate the octahedral environment of the orbitals, but they do not match the size of the actual TiO_6 octahedra.

(This figure is in colour only in the electronic version)

experimentally observed spin-wave excitation spectrum was taken as evidence for strong orbital fluctuations [14, 15]. This notion was supported also by NMR [16] and Raman studies [17]. An alternative explanation, compatible with orbital order, was proposed [12] and promptly disputed [18].

Altogether, the properties of $YTiO_3$ and related titanates are at present not fully understood and the recent studies raise a number of questions—how robust is orbital ordering in t_{2g} electron systems like $YTiO_3$, which factors determine the orbital ordering in a particular compound, can it be tuned via external parameters such as high pressure, and how does orbital order relate to other physical properties, e.g., the electronic and magnetic excitation spectra? The orbital polarizations in the rare-earth titanates manifest themselves in small distortions of the TiO_6 octahedra [11, 12] so it should be possible to obtain information on the orbital ordering from structural studies.

We investigate here the structural and electronic changes in $YTiO_3$ under high pressure. The x-ray diffraction experiments evidence distinct changes in the octahedral distortion as a function of pressure that will be discussed in terms of a pressure-driven reorientation of the Ti $3d(t_{2g})$ orbitals in $YTiO_3$. The effect of these structural/orbital changes on the electronic properties of $YTiO_3$ are investigated by determining quantitatively the reduction of the Mott–Hubbard gap under pressure using mid-infrared spectroscopy.

2. Experimental details

Angle-dispersive x-ray powder diffraction experiments were performed at the beamline ID09A of the European Synchrotron Radiation Facility in Grenoble. A fine powder was produced from an $YTiO_3$ crystal (Curie temperature $T_C = 28$ K) grown by a floating zone technique [19]. The sample was pressurized in a diamond-anvil cell using condensed nitrogen

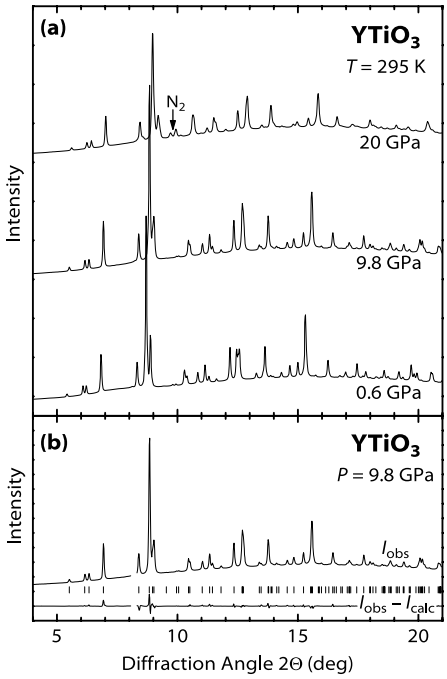

Figure 2. (a) Selected x-ray diffraction diagrams of $YTiO_3$ for pressures up to 20 GPa ($T = 295$ K, $\lambda = 0.41$ Å). (b) Rietveld refinement of data recorded at 9.8 GPa. I_{obs} and I_{calc} denote observed and calculated diffraction intensities, respectively. Markers show the calculated peak positions.

as the pressure-transmitting medium. Two-dimensional diffraction images were recorded with an image plate detector and converted to intensity-versus-2θ diffractograms (figure 2) by numerical integration [20]. The structural parameters were determined by means of Rietveld refinements [21, 22].

It is important to note that the statistical uncertainties of the diffraction intensities were calculated from the intensity variations along the individual diffraction rings, rather than assuming basic counting statistics (error proportional to the square root of the intensity). Using the experimentally determined uncertainties as weights in the Rietveld fitting process turned out to be essential for an accurate determination of the oxygen atomic positions.

Mid-infrared transmission experiments were conducted at the infrared beamline of the synchrotron ANKA in Karlsruhe. The spectra were recorded on 40 μm thick $YTiO_3$ crystals with lateral dimensions of $\sim$70–100 μm using a Bruker IFS66v/S Fourier transform spectrometer equipped with an MCT detector and a microscope. Two 15$\times$ microscope mirror objectives were used to focus the nearly diffraction-limited infrared beam onto the sample and to collect the transmitted radiation. The geometrical spot size was limited to 30 μm in diameter by appropriate field stops. Synthetic type-IIa diamond anvils (Sumitomo Electric, Japan) were used in the infrared experiments. Condensed nitrogen and solid KCl were employed as pressure media. Pressures were determined in all experiments with the ruby luminescence method [23].

3. Results and discussion

The diffraction diagrams of $YTiO_3$ (figure 2) and the measured lattice parameters (figures 3(a), (b)) change continuously with pressure. The ambient-pressure perovskite-type crystal structure

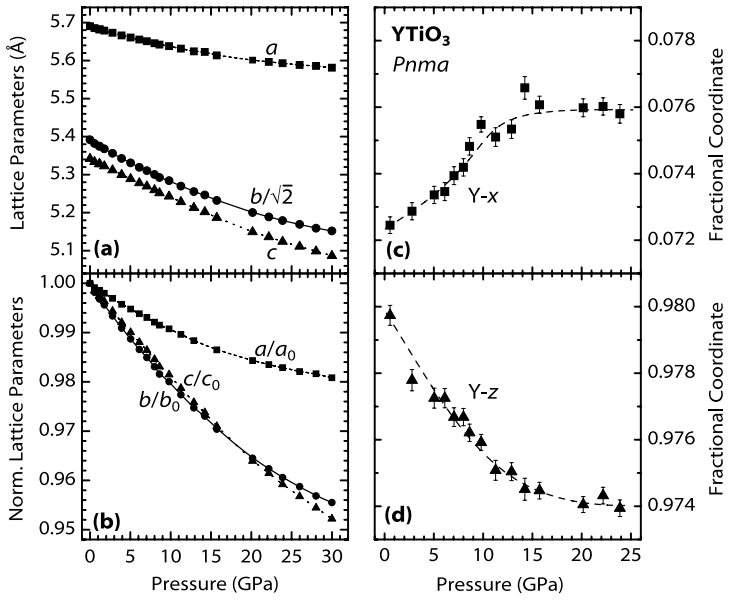

Figure 3. Structural parameters of $YTiO_3$ as a function of pressure. (a) Lattice parameters, (b) lattice parameters normalized to their respective zero-pressure values, ((c), (d)) x and z fractional coordinates of Y. The lattice parameter b was scaled by $\sqrt{2}$ in (a) to obtain a pseudo-cubic representation.

of $YTiO_3$ is thus stable under compression up to at least 30 GPa. The compressibility exhibits a distinct anisotropy with the a direction being only about half as compressible as the b and c directions (figure 3(b)); in other words, the orthorhombic strain increases with pressure. The increasing distortion is evident also from the variation of the yttrium coordinates x and z with pressure shown in figures 3(c), (d) ($y = 1/4$ by symmetry). Under pressure, the yttrium ions clearly move further away from the 'ideal' position $(0, 1/4, 1)$ in an undistorted (cubic) perovskite. This shift levels off, however, at around 15 GPa.

A Birch equation of state was fitted to the pressure–volume data up to 30 GPa to determine the bulk modulus $B_0 = 163(6)$ GPa and its pressure derivative at zero pressure $B' = 8.5(10)$; the zero-pressure volume was fixed at the measured value of $V_0 = 231.78(2)$ Å^3.

The variations of the Ti–O distances with pressure (figure 4) represent the most important structural information. At ambient pressure, the long Ti–O2(a) distance exceeds the two shorter ones by ∼3% (Ti–O2(a) and Ti–O2(b) denote the two distinct Ti–O2 distances). This type of distortion persists up to about 8 GPa. On increasing the pressure further, the initially short Ti–O2(b) distance *lengthens* with increasing pressure, while Ti–O2(a) shortens markedly. As a result, the two Ti–O2 bond lengths become (i) nearly equal at 13 GPa and (ii) distinctly larger than the Ti–O1 distance. The observation of such distinct changes in the octahedral distortion raises the question of whether and how they relate to changes in the orbital ordering.

It was discussed in previous work (see, e.g., [4, 11, 12]) that the deformation of the TiO_6 octahedra reflects the spatial orientation of the t_{2g} wavefunction in rare-earth titanates. To facilitate the discussion, we introduce a *local* coordinate system at each Ti site with the x, y, and z axes parallel to the Ti–O2(a), Ti–O2(b), and Ti–O1 bonds, respectively (figure 1). The relative Ti–O distances at 0 GPa (long along x; short along y and z) indicate nearly equal occupancy of the $|xy\rangle$ and $|xz\rangle$ orbitals. The eigenfunction thus becomes $\approx\sqrt{0.5}|xy\rangle + \sqrt{0.5}|xz\rangle$, in

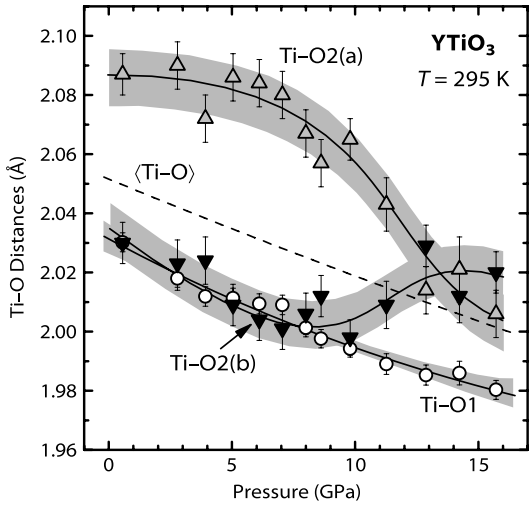

Figure 4. Ti–O bond lengths in $YTiO_3$ as a function of pressure (symbols). ⟨Ti–O⟩ denotes the average bond length (dashed line). Grey bands indicate estimated confidence bands; solid lines are guides to the eye.

agreement with the experimental results [3–6] and all theoretical studies that addressed the orbital ordering [1, 2, 9–11].

At 13 GPa, the TiO_6 octahedra are characterized by two equally long Ti–O2 bonds along x, y and a shorter Ti–O1 distance along z, i.e., the octahedra are compressed along z. Using the same argument as above, such a distortion would indicate predominant occupation of the $|xy\rangle$ orbital. The changes in the Ti–O bond lengths observed in $YTiO_3$ thus indicate the possibility of *a pressure-induced reorientation of the t_{2g} orbitals* from the initial 'tilted state' with the approximate wavefunction $\sqrt{0.5}|xy\rangle + \sqrt{0.5}|xz\rangle$ to a situation where essentially only the $|xy\rangle$ orbital is occupied, as shown in figure 1(b). This interpretation finds support in the fact that the *relative* Ti–O bond lengths in $YTiO_3$ above 13 GPa are very similar to those in $SmTiO_3$ at ambient pressure, where there is theoretical support for a predominant occupation of the $|xy\rangle$ orbitals [11]. However, a first-principles study of $YTiO_3$ on the basis of the structural results presented here concludes that an orbital reorientation does not occur [12]. We will return to this issue below.

Let us first investigate how the electronic excitation spectrum of $YTiO_3$ is affected by the structural changes under pressure. Figure 6 depicts spectra of the reciprocal transmittance $1/T$ (which is related to the absorbance $A = \log_{10}(1/T)$) for several pressures up to 16 GPa. In this representation, the optical absorption edge and its pressure-induced red shift are easily recognized. To obtain quantitative results on the red shift, we determine the energies where $1/T = 300$ (corresponding to an optical conductivity of $\sim$10 Ω^{-1} cm^{-1}). The ambient-pressure optical gap thus determined at the *onset of absorption* amounts to $\sim$5300 cm^{-1} (0.7 eV), a value that is naturally somewhat smaller than the previously reported values of 6500–8000 cm^{-1} (0.8–1.0 eV) deduced from reflectance measurements [24, 25]. The important information here is the shift of the absorption edge (figure 6(b)) rather than its absolute value. At pressures above 8 GPa, the optical bandgap decreases essentially linearly with pressure at a rate of $-145(10)$ cm^{-1} GPa^{-1} (-18 meV GPa^{-1}). On the basis of a linear extrapolation of these data, the optical gap is expected to close at a pressure in the order of 40–50 GPa.

The mid-IR optical absorption of rare-earth titanates has been attributed to an excitation across the Mott–Hubbard gap [24, 26]. The Coulomb repulsion U is not expected to change

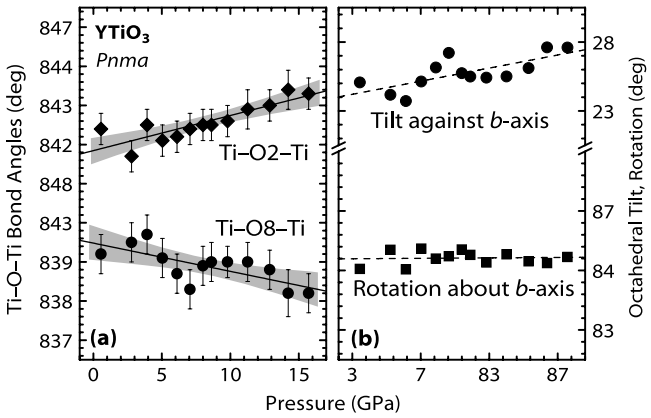

Figure 5. (a) Ti–O–Ti bond angles and (b) octahedral tilt and rotation angles in $YTiO_3$ as a function of pressure. Lines are guides to the eye; the shaded bands indicate confidence bands.

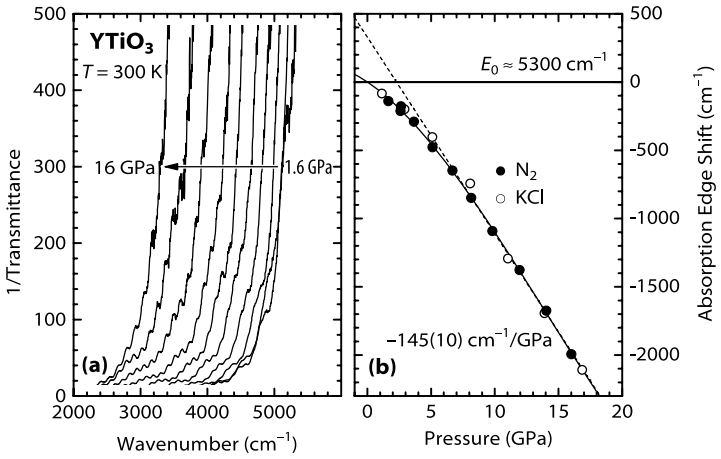

Figure 6. Mid-infrared optical absorption in $YTiO_3$ under pressure ($T = 295$ K). (a) 1/transmittance spectra recorded at pressures of 1.6, 2.6, 3.7, 5.1, 6.7, 8.2, 9.8, 12.0, 14.1, and 16.0 GPa (with the nitrogen pressure medium). The modulations of the spectra originate from interferences. (b) Pressure-induced shift of the optical absorption edge determined at 1/transmittance = 300 from two experimental runs with the condensed nitrogen and the KCl pressure medium, respectively.

under pressure, so the reduction in bandgap is a measure of the increase in bandwidth. The electronic bandwidth under pressure is usually interpreted in terms of the Ti–O bond lengths and the Ti–O–Ti bond angles. In the present case, the changes in the bond angles, i.e. $\pm 1^\circ$ up to 16 GPa, are relatively small compared to those for related perovskites like rare-earth nickelates [27] or $LaMnO_3$ [28]. In fact, the *average* bond angle is essentially pressure insensitive due to the opposite changes in the Ti–O1–Ti and Ti–O2–Ti bond angles (figure 5). Therefore, we suppose that the variation in the average Ti–O bond length d dominates the reduction of the Mott–Hubbard gap E_g under pressure. Using the results on the variation of the average Ti–O bond length with pressure (figure 4), this can be quantified in terms of a gap deformation potential, $\mathrm{d}E_g/\mathrm{d}\ln d = 11(2)$ eV in the region of linear change.

Figure 6(b) evidences a very unusual superlinear change of the optical gap with pressure: the initial slope of the absorption edge shift is only about half as large when compared to the

region above 10 GPa. The increase in slope up to ∼10 GPa can hardly be correlated with changes in the *average* bond length or the bond angles. The only distinct structural change at around 10 GPa relates to the octahedral distortion as discussed above. For comparison, we have measured also the pressure dependence of the optical gap in $LaMnO_3$ (not shown here), and it shows only the expected linear variation with volume (or a slightly sublinear one with pressure). The observation of a structural anomaly near 10 GPa and a change in the pressure dependence of the optical gap in the same pressure range brings us back to the question of a pressure-driven orbital reorientation.

To understand how pressure can in principle induce an orbital transition, one should take into account two effects that induce a splitting of the t_{2g} states. Firstly, in the presence of the $GdFeO_3$-type distortion, the crystal field of the Y ions lifts the degeneracy of the Ti t_{2g} states. This splitting will increase if the Y–Ti distances are shortened, i.e., under pressure. Secondly, a Jahn–Teller distortion due to the Ti–O interaction can modify or even dominate the energetics of the Ti t_{2g} states. Due to the stiffening of the lattice, Jahn–Teller distortions will usually become less favorable under compression [28]. Application of high pressure is thus expected to tune the balance between these two contributions, which can lead to changes in the orbital ordering. These effects have been discussed in detail before—see, e.g., [11, 12, 29], and references therein.

In terms of the *relative* Ti–O bond lengths, the situation in $YTiO_3$ at 15 GPa is very similar to that in $SmTiO_3$ at ambient pressure. In the latter case, there exists no Jahn–Teller distortion of the type encountered in $YTiO_3$; the competition between the crystal field of the rare-earth ions and that of the O ions was reported to be rather balanced [29], and $SmTiO_3$ is thought to have predominant occupation of the $|xy\rangle$ orbital [11]. The octahedral distortion observed in $YTiO_3$ above 10 GPa thus suggests a predominant occupation of the $|xy\rangle$ orbital and accordingly a pressure-driven orbital reorientation. The comparison between $YTiO_3$ and $SmTiO_3$ is also of interest with regard to magnetism. In contrast to $YTiO_3$, $SmTiO_3$ is an antiferromagnet [30]. In view of the possible orbital reorientation and the coupling between spins and orbitals, one may speculate that $YTiO_3$ becomes antiferromagnetic under pressure. $YTiO_3$ would then lose its unusual property of being simultaneously ferromagnetic *and* insulating.

A recent theoretical investigation by Pavarini *et al* [12] addresses the questions of orbital ordering, electronic bandgap and magnetism for $YTiO_3$. Their first-principles study is based on the experimental $YTiO_3$ crystal structure data presented here. These calculations do not support the notion of an orbital reorientation. If the calculations capture the pressure-induced changes in $YTiO_3$ correctly, it would imply that above 10 GPa the nearest-neighbor Ti–O interactions are too weak to stabilize an octahedral distortion that corresponds to the orbital ordering of the Ti 3d electrons. Presumably, the Y–O interaction would contribute significantly to determining the octahedral distortion. The measured variations of the Y–O distances with pressure (not shown here) yield, however, no direct explanation for the change in the octahedral distortion at ∼10 GPa. Altogether, this scenario would be very different from the ambient-pressure situation, where the octahedral distortions in the rare-earth titanates generally reflect the orbital order.

It is not clear at present to what extent the first-principles calculations of [12] fully capture the essence of the pressure-induced changes in $YTiO_3$. These calculations predict a metallization pressure in the order of ∼100 GPa, which is more than two times larger than the experimental estimate. In addition, the calculated bandwidth as a function of pressure does not exhibit any features that would correspond to the experimentally observed change in slope in the pressure dependence of the optical gap (figure 6(b)). It would therefore be an important test to check whether first-principles calculations in the spirit of [12] are able to reproduce the pressure-induced changes in the octahedral distortion (rather than using it as a starting point).

Further experimental and theoretical work is required to arrive at a definite conclusion as regards whether the changes in the octahedral distortion observed here are indeed related to an orbital reorientation. Should such a pressure-induced reorientation be confirmed, it would open the way to studying the important question of how orbital order relates to other physical properties in a given system, i.e., without chemical modification.

4. Conclusions

The pressure-induced structural changes in $YTiO_3$ were studied in detail by means of synchrotron x-ray diffraction. Distinct changes in the distortion of the TiO_6 octahedra were observed at around 10 GPa, and a spatial reorientation of the occupied Ti $3d(t_{2g})$ orbitals has been discussed as a possible explanation. The combination of infrared transmission and x-ray diffraction experiments made it possible to obtain direct, quantitative information on the change of the electronic bandgap/bandwidth for a rare-earth transition metal perovskite together with a detailed knowledge of the associated structural changes. The present results provide a basis for further experimental and theoretical work on the issue of a pressure-induced orbital reorientation in $YTiO_3$ as well as a framework for testing theoretical models of the electronic structure of the t_{2g} band titanates in the vicinity of the insulator–metal borderline.

Acknowledgments

We acknowledge the stimulating discussions with O K Andersen, K Held, and A Yamasaki. We thank F X Zhang for support in the early stage of this study and M Süpfle for technical support at ANKA.

References

[1] Sawada H and Terakura K 1998 *Phys. Rev.* B **58** 6831
[2] Mizokawa T and Fujimori A 1996 *Phys. Rev.* B **54** 5368
[3] Itoh M, Tsuchiya M, Tanaka H and Motoya K 1999 *J. Phys. Soc. Japan* **68** 2783
[4] Akimitsu J, Ichikawa H, Eguchi N, Miyano T, Nishi M and Kakurai K 2001 *J. Phys. Soc. Japan* **70** 3475
[5] Nakao H, Wakabayashi Y, Kiyama T, Murakami Y, Zimmermann M v, Hill J P, Gibbs D, Ishihara S, Taguchi Y and Tokura Y 2002 *Phys. Rev.* B **66** 184419
[6] Iga F, Tsubota M, Sawada M, Huang H B, Kura S, Takemura M, Yaji K, Nagira M, Kimura A, Jo T, Takabatake T, Namatame H and Taniguchi M 2004 *Phys. Rev. Lett.* **93** 257207
[7] Tsubota M, Igay F, Uchihira K, Nakano T, Kura S, Takabatake T, Kodama S, Nakao H and Murakami Y 2005 *J. Phys. Soc. Japan.* **74** 3259
[8] Kubota M, Nakao H, Murakami Y, Taguchi Y, Iwama M and Tokura Y 2004 *Phys. Rev.* B **70** 245125
[9] Mizokawa T, Khomskii D I and Sawatzky G A 1999 *Phys. Rev.* B **60** 7309
[10] Pavarini E, Biermann S, Poteryaev A, Lichtenstein A I, Georges A and Andersen O K 2004 *Phys. Rev. Lett.* **92** 176403
[11] Mochizuki M and Imada M 2004 *New J. Phys.* **6** 154
[12] Pavarini E, Yamasaki A, Nuss J and Andersen O K 2005 *New J. Phys.* **7** 188
[13] Solovyev I V 2006 *Phys. Rev.* B **73** 155117
[14] Ulrich C, Khaliullin G, Okamoto S, Reehuis M, Ivanov A, He H, Taguchi Y, Tokura Y and Keimer B 2002 *Phys. Rev. Lett.* **89** 167202
[15] Khaliullin G and Okamoto S 2002 *Phys. Rev. Lett.* **89** 167201
[16] Kiyama T, Saitoh H, Itoh M, Kodama K, Ichikawa H and Akimitsu J 2005 *J. Phys. Soc. Japan* **74** 1123
[17] Ulrich C, Gossling A, Gruninger M, Guennou M, Roth H, Cwik M, Lorenz T, Khaliullin G and Keimer B 2006 *Phys. Rev. Lett.* **97** 157401
[18] Khaliullin G 2005 *Prog. Theor. Phys. Suppl.* **160** 155

[19] Cwik M, Lorenz T, Baier J, Müller R, André G, Bourée F, Lichtenberg F, Freimuth A, Schmitz R, Müller-Hartmann E and Braden M 2003 *Phys. Rev.* B **68** 060401(R)
[20] Hammersley A 1998 *Computer Program Fit2D* ESRF, Grenoble
[21] Larson A C and von Dreele R B 1986 GSAS: general structure analysis system *Report LAUR 86-748* Los Alamos National Laboratory, NM, USA
[22] Toby B H 2001 *J. Appl. Crystallogr.* **34** 210 (computer program EXPGUI)
[23] Piermarini G J, Block S, Barnett J D and Forman R A 1975 *J. Appl. Phys.* **46** 2774
Mao H K, Xu J and Bell P M 1986 *J. Geophys. Res.* **91** 4673
[24] Arima T, Tokura Y and Torrance J B 1993 *Phys. Rev.* B **48** 17006
[25] Okimoto Y, Katsufuji T, Okada Y, Arima T and Tokura Y 1995 *Phys. Rev.* B **51** 9581
[26] Crandles D A, Timusk T, Garret J D and Greedan J E 1992 *Physica* C **201** 407
[27] Amboage M 2003 *PhD Thesis* University of the Basque Country, Bilbao, Spain
[28] Loa I, Adler P, Grzechnik A, Syassen K, Schwarz U, Hanfland M, Rozenberg G K, Gorodetsky P and Pasternak M P 2001 *Phys. Rev. Lett.* **87** 125501
[29] Mochizuki M and Imada M 2004 *J. Phys. Soc. Japan* **73** 1833
[30] Katsufuji T, Taguchi Y and Tokura Y 1997 *Phys. Rev.* B **56** 10145
[31] MacLean D A, Ng H-N and Greedan J E 1979 *J. Solid State Chem.* **30** 35